Journal of Solid State Chemistry 183 (2010) 1905–1911

Contents lists available at ScienceDirect

Journal of Solid State Chemistry

journal homepage: www.elsevier.com/locate/jssc

Synthesis, structures and magnetic properties of pseudo-hollandite chromium sulfides

Satoshi Yamazaki *, Yutaka Ueda

Materials Design and Characterization Laboratory, Institute for Solid State Physics, University of Tokyo, 5-1-5 Kashiwanoha, Kashiwa, Chiba 277-8581, Japan

ARTICLE INFO

Article history:
Received 3 December 2009
Received in revised form
2 March 2010
Accepted 8 March 2010
Available online 7 April 2010

Keywords:
ACr_5S_8
Pseudo-hollandite chromium sulfides
Synthesis and crystal structure
Magnetic properties

ABSTRACT

The pseudo-hollandite chromium sulfides, ACr_5S_8 (A=K, Rb, Cs) and $A'_{0.5}Cr_5S_8$ (A'=Sr, Ba), have been synthesized and investigated in structural and magnetic properties. All the compounds crystallize in the isostructure with a monoclinic $C2/m$. Its crystal structure has triangular lattices and double chains made of Cr^{3+} (d^3; S=3/2) triangles. The magnetic susceptibilities of all compounds behave as Curie–Weiss types in high temperature region. From magnetic susceptibility and specific heat measurements, all the compounds have antiferromagnetic ground states. The Néel temperatures are rather low compared to Weiss temperatures, reflecting magnetic frustration in the triangular lattices and double chains. The magnetic transitions in KCr_5S_8 and $Ba_{0.5}Cr_5S_8$ are a two-step transition around 50 and 60 K, respectively, while $RbCr_5S_8$ shows a sharp magnetic transition at 42 K, accompanied by magnetoelastic behavior. $CsCr_5S_8$ shows a structural transition around 100 K, followed by a magnetic transition at 10 K. In $Sr_{0.5}Cr_5S_8$, ferromagnetic interaction develops below 100 K and then a three-dimensional antiferromagnetic order takes place at 30 K. These magnetic properties are discussed from A-cation dependences of local structures and a model of magnetic structure for $RbCr_5S_8$ is proposed on the basis of the arguments of magnetic interactions and neutron diffraction data. It is different from the known magnetic structure of $TlCr_5Se_8$.

1. Introduction

There exist many ternary chalcogenides, $A_xM_yX_z$ (A=Tl, alkaline and alkaline-earth elements; M=transition metals; X=S, Se, Te) with two-dimensional (2D) layer-type and/or one-dimensional (1D) tunnel-type frameworks formed by M_yX_z, where A-cations reside in interlayers and/or tunnels and act as electron donors to the M_yX_z frameworks. These compounds have provided playgrounds of interesting conductive and magnetic properties. Especially, the discovery of superconductivity in $Tl_xV_6S_8$ with a tunnel structure has accelerated the study on vanadium compounds [1,2]. In such current of study, the first pseudo-hollandite chalcogenide, TlV_5S_8 was reported by Fournès et al. [3]. Since the report of TlV_5S_8, many pseudo-hollandite chalcogenides, particularly A=Tl compounds, have been prepared and investigated in the structure and physical properties. TlV_5S_8 and TlV_5Se_8 are metals [4,5]. On the other hand, $TlCr_5S_8$ and $TlCr_5Se_8$ are semiconductors and antiferromagnetically order below Néel temperatures T_N=50 K and 55 K, respectively [6,7]. ACr_5S_8 (A=K, Rb and Cs) and $Ba_{0.5}Cr_5S_8$ were also synthesized by Huster [8]. $Sr_{0.5}Cr_5S_8$ was synthesized by Petricek et al. [9].

The pseudo-hollandite chalcogenides have a general chemical formula of $A_xM_5X_8$. Its monoclinic structure with a space group $C2/m$ is shown in Fig. 1, taking chromium sulfide, ACr_5S_8, as an example [8]. In the structure there are three crystallographically independent Cr sites, Cr(1), Cr(2) and Cr(3), and all Cr atoms are coordinated by six sulfur atoms to form CrS_6 octahedron. Cr(1)S_6 and Cr(2)S_6 octahedra form 2D triangular lattices by sharing the edges of octahedra. On the other hand, Cr(3)S_6 octahedra form 1D double chains (zigzag chains) by sharing the edges of octahedra, and the double chains bridge the triangular lattices by sharing the faces of Cr(2)S_6 and Cr(3)S_6 octahedra. Consequently, thus formed Cr_5S_8 framework has tunnels and A-cations occupy the tunnel sites each of which is coordinated by ten sulfur atoms.

Many pseudo-hollandit chromium chalcogenides have been synthesized; nevertheless there has been no report on the detailed structures and physical properties of chromium compounds except for $TlCr_5S_8$ and $TlCr_5Se_8$. Cr ion takes Cr^{3+} (d^3, S=3/2) state without orbital degree of freedom in these compounds. Hence we can expect any frustration in antiferromagnetic ordering or any competition between antiferromagnetic and ferromagnetic interactions, because the pseudo-hollandite structure has 2D triangular lattice and double chain (1D zigzag chain) both of which are constructed by triangles of Cr^{3+}. This paper reports the synthesis, structures and magnetic properties of ACr_5S_8 (A=K, Rb and Cs) and $A'_{0.5}Cr_5S_8$ (A'=Sr and Ba).

* Corresponding author. Fax: +81 471 3436.
E-mail address: satoshi@issp.u-tokyo.ac.jp (S. Yamazaki).

0022-4596/$ - see front matter © 2010 Elsevier Inc. All rights reserved.
doi:10.1016/j.jssc.2010.03.013

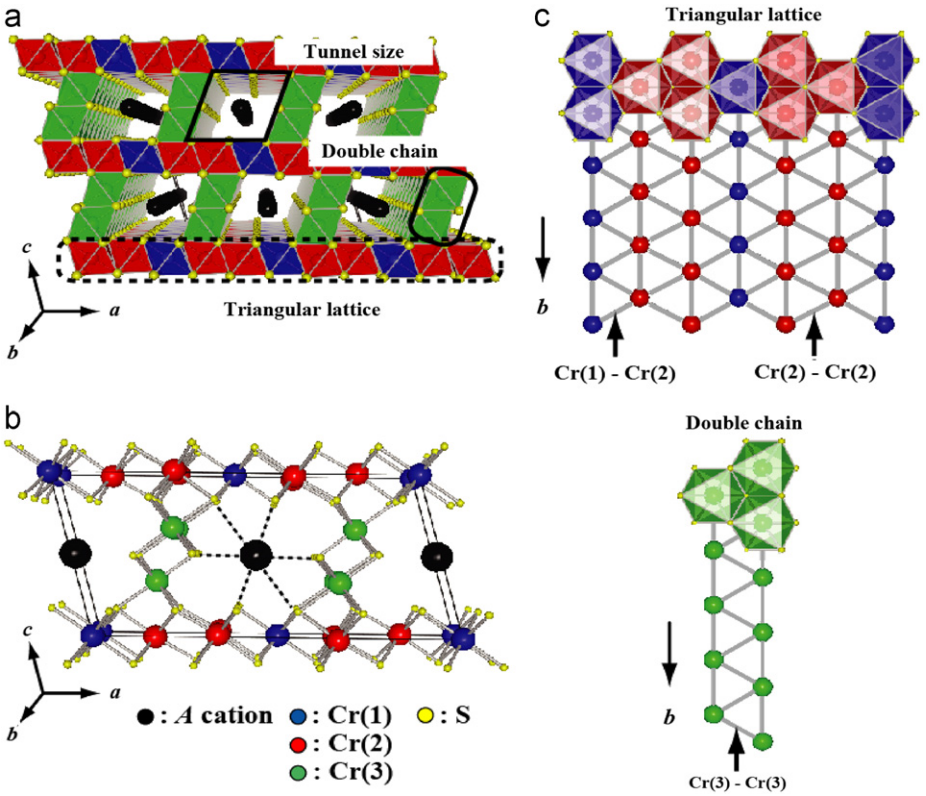

Fig. 1. The pseudo-hollandite structure of ACr_5S_8 drawn on the structural data obtained from Ref. [8]. (a) A schematic illustration viewed from *b*-direction, (b) coordination manners and (c) schematic illustrations of triangular lattice and double chain made up of edge-sharing CrS_6 octahedra. There are three Cr sites; Cr(1), Cr(2) and Cr(3), with each distance of Cr(1)–Cr(2), Cr(2)–Cr(2) and Cr(3)–Cr(3). The $Cr(1)S_6$, $Cr(2)S_6$ and $Cr(3)S_6$ octahedra are represented by blue, red and green colors, respectively. (For interpretation of the references to color in this figure legend, the reader is referred to the web version of this article.)

All the compounds have antiferromagnetically ordered ground states with rather lower Néel temperatures than Weiss temperatures, reflecting strong frustration effect. Furthermore, they show a variety of magnetic transitions, depending on *A*-cations. The magnetic properties will be discussed in terms of *A*-cation dependence of local structures. A model of magnetic structure for $RbCr_5S_8$ is also proposed.

2. Experimental

Powder samples were synthesized by a solid state reaction of elements; alkaline metals (K, Rb and Cs), alkaline-earth metals (Sr and Ba), chromium metal (Cr) and sulfur (S). Since alkaline and alkaline-earth metals are unstable and active under ordinary atmosphere with moisture, all procedures of sample preparation were done in a dry box filled with Ar gas as follows: Weigh each element, pack weighed elements into a silica capsule in the order of alkaline or alkaline-earth metals, Cr and S, and seal the capsule into a silica tube with Ar gas. The thus sealed silica tubes were heated at 160 K for 24 h after gradual elevation of temperature up to 160 K, taking 12 h. In this process, the starting elements are uniformly mixed in melted sulfur and gradually react with sulfur. Next, the temperature was elevated up to 713 K, taking over 12 h and they were heated at 713 K for 24 h. During this process, sulfur completely reacts with metal elements to form any sulfides. Finally the temperature was elevated up to 1027 K and held at 1027 K for six days to make well crystallized samples, and then slowly lowered to room temperature. The reaction process without holding at 160 and 713 K always gave the inclusion of impurity Cr_2S_3.

The obtained samples were characterized to be single phase by powder X-ray diffraction (XRD) using MXP21 Mac Science diffractometer with Cu*K*α radiation $\lambda = 1.5405$ Å. The stoichiometry of samples was checked by energy-dispersive X-ray analysis (EDX) and electron diffraction (ED) in transmission electron microscope (TEM) experiments using JEOL-EM2010 operated at 200 kV. Any diffusive ED caused from *A*-cation off-stoichiometry was not observed and EDX gave almost the stoichiometric ratio of $A(A'):Cr:S = 1 \pm 0.02(0.5 \pm 0.01):5 \pm 0.02:8$ in all samples. The ordering of Ba or Sr along the *b*-axis in $A'_{0.5}Cr_5S_8$ was confirmed from the observations of (0 1/2 0) reflection in ED and of the lattice image in TEM.

The magnetic susceptibility was measured in an external magnetic field of $H = 1.0$ T from 5 to 350 K on heating after zero-field cooling with a superconducting quantum interference device (SQUID) magnetometer (Quantum Design MPMS XL). Specific heat data were collected by means of a pulse relaxation method using a commercial calorimeter (Quantum Design PPMS) from 2 to 300 K. Powder neutron diffraction (ND) measurements were conducted using a triple-axis spectrometer, HQR, installed at the guide hall of JRR-3M in JAERI. Neutrons with a wavelength of 2.45508 Å were used.

3. Results

3.1. A-cation dependences of the structure

Among alkaline and alkaline-earth elements, K, Rb, Cs, Sr and Ba formed pseudo-hollandite chromium compounds, while Na and Ca did not. Fig. 2 shows powder XRD pattern of $RbCr_5S_8$ and its Rietveld analysis, as a representative of a series compounds.

All the compounds crystallized in the isostructure with a monoclinic $C2/m$. The structural data were obtained from Rietveld analysis of these XRD patterns using the program RIETAN [10]. Fig. 3 shows the lattice parameters at room temperature as a function of A-cation radius. The larger the A-cation radius is, the larger all the lattice parameters are except β. The tunnel size also increases with increase of A-cation radius. In the compounds with tunnels, guest ions with larger ionic radii tend to hardly form compounds. In the pseudo-hollandite chromium sulfides, however, Na^+ and Ca^{2+} with smaller ionic radii than Sr^{2+} did not form the compound. This is probably because small ions cannot screen the charged $[Cr_5S_8]^{-1}$ framework effectively.

On the other hand, the local structures do not show general trend in the A-cation dependences, as seen in Fig. 4(a). Cr(1)–Cr(2) and Cr(3)–Cr(3) distances increase with increase of A-cation radii, while Cr(2)–Cr(2) and Cr(2)–Cr(3) distances show a minimum at $Ba_{0.5}Cr_5S_8$, or rather, those of $Sr_{0.5}Cr_5S_8$ are anomalously large. The difference of these Cr–Cr distances significantly affects the degree of distortion of triangles formed by Cr ions. The triangular lattice is originally composed by Cr(2)–Cr(2) double chains and Cr(1) single chains, as shown in Fig. 1(c), and it consists of two kinds of equilateral triangles with the common distance (b-axis); one ($t-1$) has two short (Cr(1)–Cr(2)) and one long (b-axis) distances, and the other ($t-2$) has two long (Cr(2)–Cr(2)) and one short (b-axis) distances. The double chain is also constructed by equilateral triangles ($t-3$) with two short (Cr(3)–Cr(3)) and one long (b-axis) distances, as shown in Fig. 1(c). The order of the length is Cr(1)–Cr(2)∼Cr(3)–Cr(3) < b-axis < Cr(2)–Cr(2) in all compounds. The degree of the distortion of triangles defined as $R_1=l_{Cr1}/l_b$, $R_2=l_b/l_{Cr2}$ and $R_3=l_{Cr3}/l_b$, where l_{Cr1}, l_{Cr2}, l_{Cr3} and l_b are the lengths of Cr(1)–Cr(2), Cr(2)–Cr(2), Cr(3)–Cr(3) and the b-axis, respectively, is also shown in Fig. 4(b). The triangles, $t-1$ for all compounds and $t-3$ except for $Sr_{0.5}Cr_5S_8$, are rather close to regular triangles, while those, $t-2$ for all compounds and $t-3$ for $Sr_{0.5}Cr_5S_8$, are distorted, particularly the $t-2$ for $Sr_{0.5}Cr_5S_8$ is heavily distorted. The long Cr(2)–Cr(2) distance allows us to regard the triangular lattice as Cr(2)–Cr(1)–Cr(2) hexagonal chains joined each other with long Cr(2)–Cr(2) distance (Fig. 1(c)). Particularly, such feature is remarkable in $Sr_{0.5}Cr_5S_8$. The Cr(2)–Cr(1)–Cr(2) hexagonal chain formed by the triangles ($t-1$) with R_1 consists of slightly distorted hexagons elongated along the b-axis. These structural characteristics are important to discuss the magnetic properties and magnetic structures. They will be discussed in the Section 4.

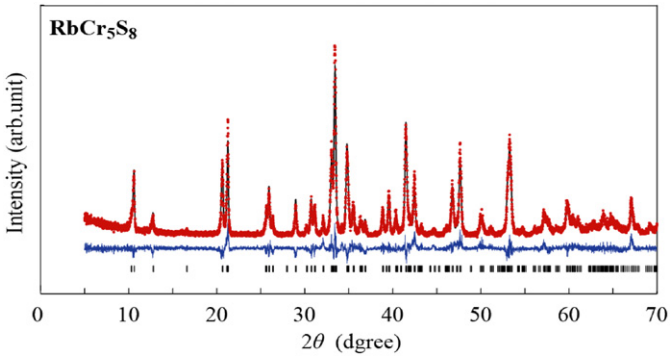

Fig. 2. Powder X-ray diffraction pattern of $RbCr_5S_8$ at room temperature and its Rietveld analysis. The dots: raw data, the line: calculation, the medium: difference between raw data and calculation and the bottom: positions of diffraction peaks. The *Rwp*-value is 9%.

3.2. Magnetic properties

All the compounds are insulators. The temperature dependences of magnetic susceptibilities $\chi(T)$ and specific heat of the compounds are shown in Figs. 5 and 6, respectively. The $\chi(T)$ of all compounds

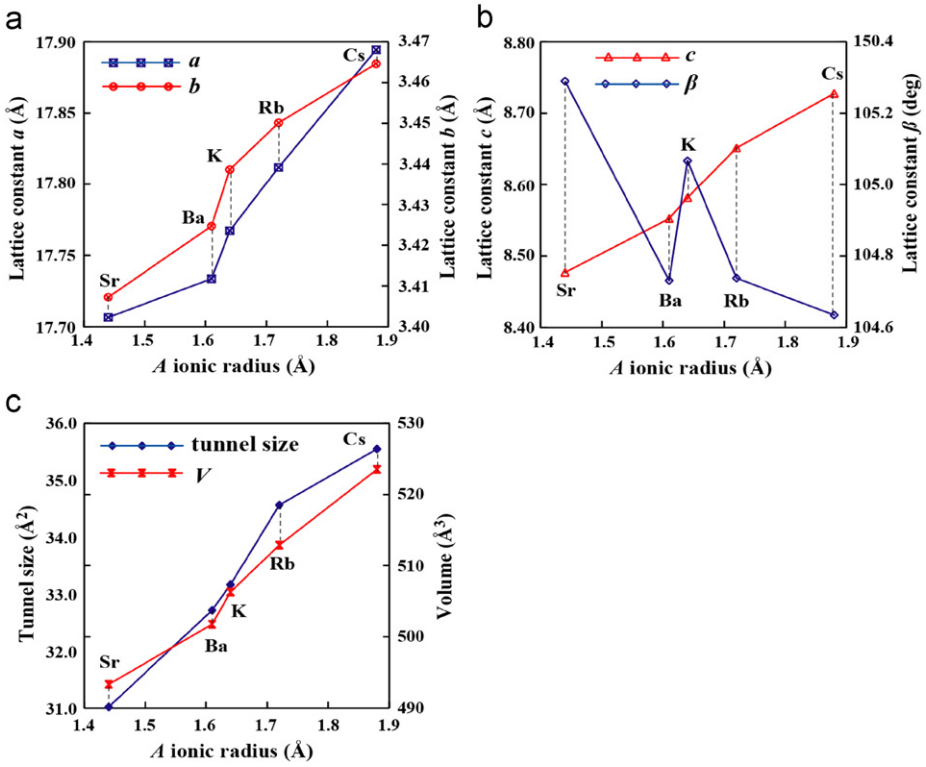

Fig. 3. Lattice parameters of ACr_5S_8 (A=K, Rb, Cs) and $A'_{0.5}Cr_5S_8$ (A'=Sr, Ba) at room temperature as a function of A-cation radius: (a) a-axis and b-axis, (b) c-axis and β-angle and (c) tunnel size and volume.

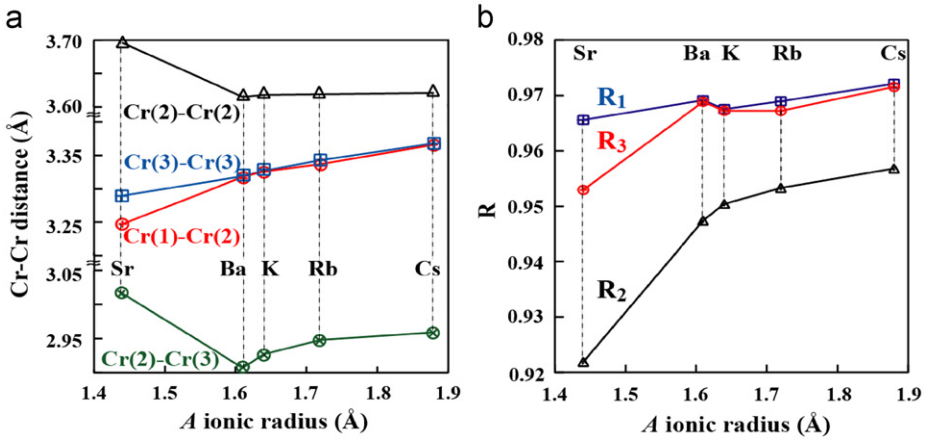

Fig. 4. *A*-cation dependences of (a) Cr–Cr distances and (b) the distortion of triangles defined as $R_1=l_{Cr1}/l_b$, $R_2=l_b/l_{Cr2}$ and $R_3=l_{Cr3}/l_b$, where l_{Cr1}, l_{Cr2}, l_{Cr3} and l_b are the distances of Cr(1)–Cr(2), Cr(2)–Cr(2), Cr(3)–Cr(3) and the *b*-axis, respectively.

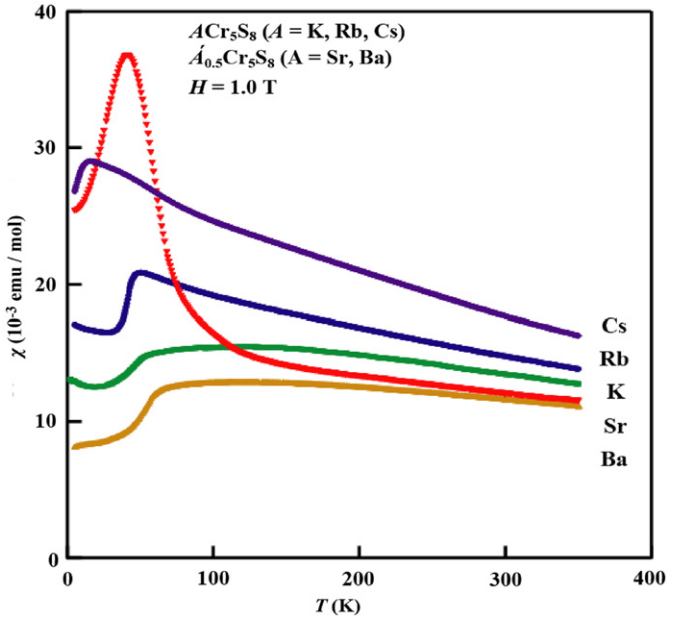

Fig. 5. Temperature dependences of magnetic susceptibilities for ACr_5S_8 (A=K, Rb, Cs) and $A'_{0.5}Cr_5S_8$ (A'=Sr, Ba) measured under H=1.0 T.

show Curie–Weiss (CW) behaviors in high-temperature region, but the behaviors in low-temperature region are rather different among the compounds. The effective moments, μ_{eff}, obtained from Curie constants and Weiss temperatures, θ_W, are listed in Table 1. The values of μ_{eff} are within the range of 3.9–4.1μ_B/Cr-atom, which are close to the spin-only value of 3.87μ_B for Cr^{3+} (S=3/2).

The $\chi(T)$ of KCr_5S_8 shows a broad maximum centered at 120 K, suggesting a low-dimensional nature in magnetism, and it shows the reduction below 55 K. The compound ($Ba_{0.5}Cr_5S_8$) of Ba^{2+} with a comparable ionic radius to K^+ shows a similar low-dimensional behavior and the reduction of $\chi(T)$ below 60 K. To confirm antiferromagnetic transitions at 55 K for KCr_5S_8 and 60 K for $Ba_{0.5}Cr_5S_8$, specific heat was measured. Unexpectedly, the specific heat curves show double peaks at T_N and T_N' in the narrow temperature region around 55 K for KCr_5S_8 (not shown) and 60 K for $Ba_{0.5}Cr_5S_8$ as shown in Fig. 6(a). This indicates that the magnetic transition occurs in two steps in both compounds. The roughly estimated entropy change of 9.8 (J/Kmol) by subtracting the background from raw data is close to magnetic entropy change $\Delta S=R\ln(2S+1)=11.5$ (J/Kmol) of Cr^{3+} in both compounds. In the present study, the background curve (the contribution of lattice) has been obtained by incorporating three Debye-type and one Einstein-type contributions; Cb=xCD1+yCD2+(14−x−y)CE, where CD1 and CD2 are from Debye-type phonons characterized by Debye temperatures Θ_{D1} and Θ_{D2} and CE is from an Einstein-type phonon with an Einstein temperature Θ_E, because there is no nonmagnetic reference compound from which the contribution of lattice can be estimated. The background curves for other compounds have been estimated by the same method. The ratio of ΔS at the two transitions is roughly 2(T_N) to 3(T_N'). This ratio is coincident with the ratio of the number of Cr^{3+} ions in the double chains to that in the triangular lattices. Therefore the double transitions might be explained as that a long range magnetic ordering suppressed by magnetic frustration in the triangular lattices is triggered by the development of magnetic order in the double chains.

In $RbCr_5S_8$, $\chi(T)$ shows a CW behavior in a rather wide range of temperature and sharply decreases below 50 K (Fig. 5). Such sharp reduction of $\chi(T)$ suggests any correlation between magnetism and lattice. However, ED and powder XRD at low temperatures revealed no evidence for structural change. Instead the temperature dependence of lattice parameters turns to an increase below 50 K from a decrease on cooling above 50 K (Fig. 7). On the other hand, a sharp peak of specific heat has been observed at 42 K (Fig. 6(b)). The estimated entropy change of ΔS=10.8 (J/Kmol) is very close to the magnetic entropy of Cr^{3+}. These results indicate that $RbCr_5S_8$ has an antiferromagnetic order at 42 K, accompanied by a magnetoelastic behavior. Such negative thermal expansion behavior has been often observed in ferromagnets, so-called invar effect, but is very rare in antiferromagnets. In this compound, it has been tried to determine the magnetic structure from powder ND, as a representative of a series compounds. Fig. 8 shows a part of ND pattern at 12 K (below T_N). Comparing to the diffraction pattern at 70 K (above T_N), many magnetic peaks are observed and the temperature dependence of intensity for these peaks clearly shows T_N=42 K (not shown). The magnetic peaks can be indexed in a monoclinic cell with a superlattice of $2\times2\times2$. This superlattice is different from that ($1\times1\times2$) of $TlCr_5Se_8$ which is a unique compound with known magnetic structure [11]. A possible magnetic structure model will be proposed and discussed in following section.

The $\chi(T)$ of $CsCr_5S_8$ increases more steeply below 100 K and shows a peak around 15 K, as shown in Fig. 5. The specific heat curve shows peaks around 100 and 10 K (Fig. 6(c)). The transition at 10 K is assigned to an antiferromagnetic transition because the

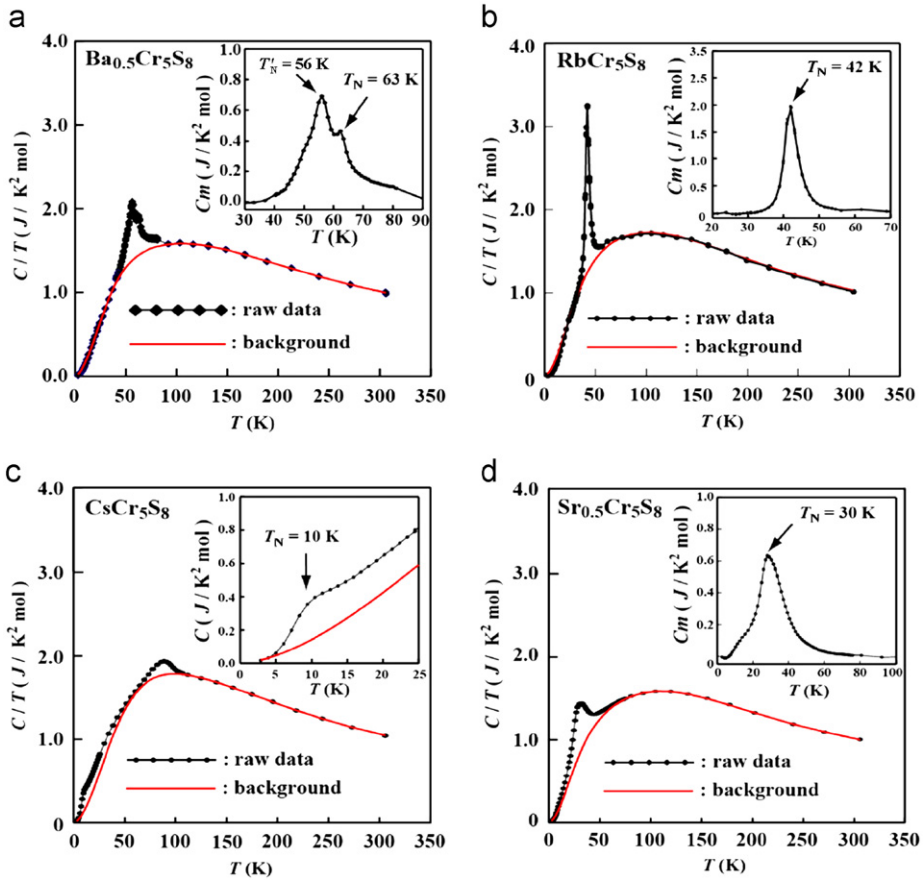

Fig. 6. Specific heat data for (a) $Ba_{0.5}Cr_5S_8$, (b) $RbCr_5S_8$, (c) $CsCr_5S_8$ and (d) $Sr_{0.5}Cr_5S_8$. The insets show specific heat obtained by subtracting the backgrounds from the raw data.

Table 1
Magnetic parameters for ACr_5S_8 (A=K, Rb, Cs) and $A'_{0.5}Cr_5S_8$ (A'=Sr, Ba).

Compound	μ_{eff}	θ_W (K)	T_N (K)	$f=\lvert\theta_W\rvert/T_N$
$Sr_{0.5}Cr_5S_8$	4.15	−680	30	22.7
$Ba_{0.5}Cr_5S_8$	4.12	−650	63	10.3
KCr_5S_8	4.10	−564	55	10.3
$Rb_{0.5}Cr_5S_8$	4.06	−442	42	10.5
$Cs_{0.5}Cr_5S_8$	3.95	−283	10	28.3

μ_{eff}: effective magnetic moment, θ_W: Weiss temperature, T_N: Néel temperature and $f=|\theta_W|/T_N$: frustration factor.

$\chi(T)$ shows a peak around the temperature. To confirm any structural change around 100 K, powder XRD was measured as a function of temperature. The obtained temperature dependences of lattice parameters are shown in Fig. 9. No change of crystal symmetry was observed down to 10 K, but an anomalous increase of the b-axis was observed around 100 K on cooling. The c-axis suddenly stops decreasing on cooling at 110 K and becomes constant below the temperature, while the a-axis and β-angle smoothly decrease with decreasing temperature. These results indicate any structural transition around 100 K. The transition has a similar aspect to that in $RbCr_5S_8$, but the thermal expansion is large and anisotropic in $CsCr_5S_8$. Although it has been still unclear whether this structural transition is accompanied by any magnetic transition or not, no drastic change of $\chi(T)$ indicates the absence of magnetic transition around 100 K.

The $\chi(T)$ of $Sr_{0.5}Cr_5S_8$ sharply increases below 100 K and shows a peak around 40 K (Fig. 5). The specific heat measurements indicate the absence of magnetic order at 100 K and the presence of an antiferromagnetic order at around 30 K (Fig. 6(d)). In $Sr_{0.5}Cr_5S_8$, ferromagnetic interaction develops below 100 K and then a three-dimensional antiferromagnetic order takes place at around 30 K. This ferromagnetic like enhancement of $\chi(T)$ will be discussed from the structural characteristics in following section.

4. Discussion

The obtained magnetic parameters are summarized in Table 1. All the compounds exhibit long range antiferromagnetic orders. The Néel temperatures (T_N) are rather low compared with Weiss temperatures (θ_W). The ratio, $f=|\theta_W|/T_N$ exceeds 10 in all compounds (Table 1). Such a suppression of T_N could be due to strong magnetic frustration in the triangle-based structure and/or the competition of ferromagnetic and antiferromagnetic interactions. In this section, we discuss magnetic interactions on the basis of the structural characteristics and propose a possible magnetic structure for $RbCr_5S_8$, as shown in Fig. 10. Here, it should be noted again that the magnetic unit cell of $RbCr_5S_8$ has a supercell of $2\times2\times2$, namely the doubling of a-, b- and c-axis. As described already, the triangular lattice can be regarded as the Cr(2)–Cr(1)–Cr(2) hexagonal chains joined by long Cr(2)–Cr(2) bonds (Fig. 1(c)). According to the literatures for chromium chalcogenides and chromium spinels with CrX_6 octahedra (X=S, Se) connected by common edges [12,13], antiferromagnetic exchange occurs for Cr–Cr=3.38 Å and exchange becomes ferromagnetic at about 3.52 Å. This can be explained from the Goodenough–Kanamori rules [14,15]. Therefore, it can be considered in the present compounds that the Cr(1)–Cr(2) bond has an antiferromagnetic

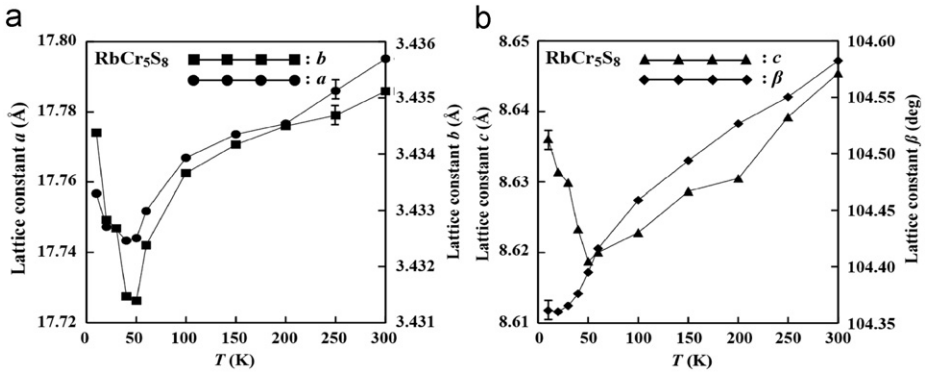

Fig. 7. Temperature dependences of lattice parameters for $RbCr_5S_8$: (a) a-axis and b-axis and (b) c-axis and β-angle.

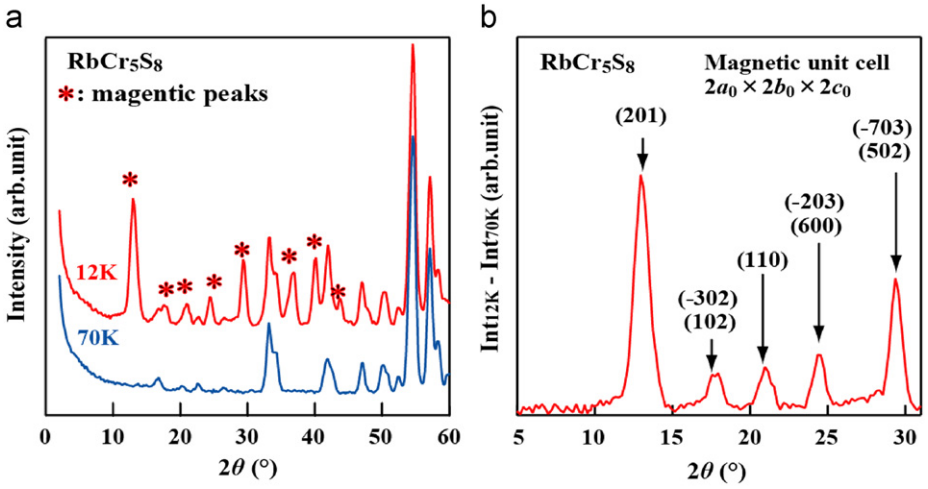

Fig. 8. (a) Neutron diffraction patterns of $RbCr_5S_8$ at 70 K ($>T_N$) and 12 K ($<T_N$). (b) Magnetic peaks obtained by subtracting the diffraction at 70 k from that at 12 K. The magnetic peaks can be indexed in a supercell of $2a_0 \times 2b_0 \times 2c_0$, where a_0, b_0 and c_0 denote the primitive cell.

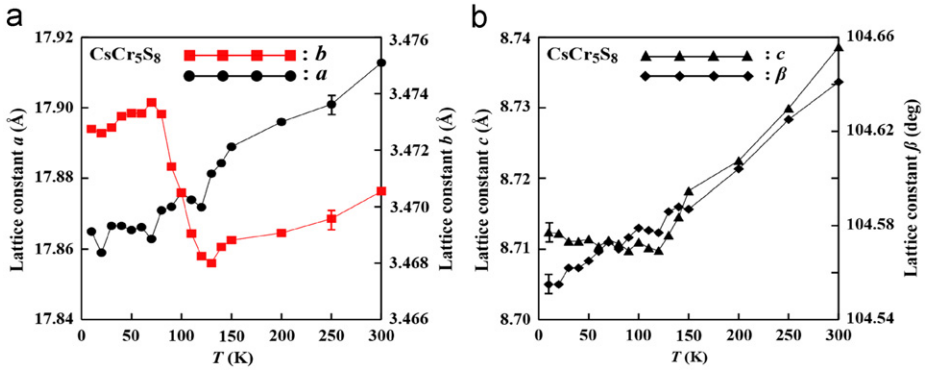

Fig. 9. Temperature dependences of lattice parameters for $CsCr_5S_8$: (a) a- and b-axis and (b) c-axis and β-angle.

interaction while the Cr(2)–Cr(2) bond has a ferromagnetic interaction (see Fig. 3). Hence, the Cr(2)–Cr(2) double chains could be ferromagnetic chains. The interaction along the b-axis with the intermediate distance is possibly antiferromagnetic. Under a dominant antiferromagnetic interaction along the b-axis, the frustration occurs in the hexagonal chain and consequently the Cr(1) chain might become an antiferromagnetic chain sandwiched by the ferromagnetic Cr(2) chains which are antiferromagnetically coupled with each other, as seen in Fig. 10. This manner requires the doubling of the b-axis in an antiferromagnetic order, as observed in $RbCr_5S_8$. Furthermore, since the face shared Cr(2)–Cr(3) bond with short distance mediates an antiferromagnetic interaction, the Cr(3) chain becomes a ferromagnetic chain antiferromagnetically coupled with the ferromagnetic Cr(2) chain, and the antiferromagnetic Cr(3)–Cr(3) bonds make the Cr(3) double chain of antiferromagnetically coupled ferromagnetic Cr(3) chains, as shown in Fig. 10. This manner requires the doubling of the c-axis from the arrangement of Cr(2)(up)–Cr(3)(down)–Cr(3)(up)–Cr(2)(down) (see Fig. 10), which is also in agreement with the observation in $RbCr_5S_8$. The doubling of the a-axis observed in $RbCr_5S_8$ is easily modeled by

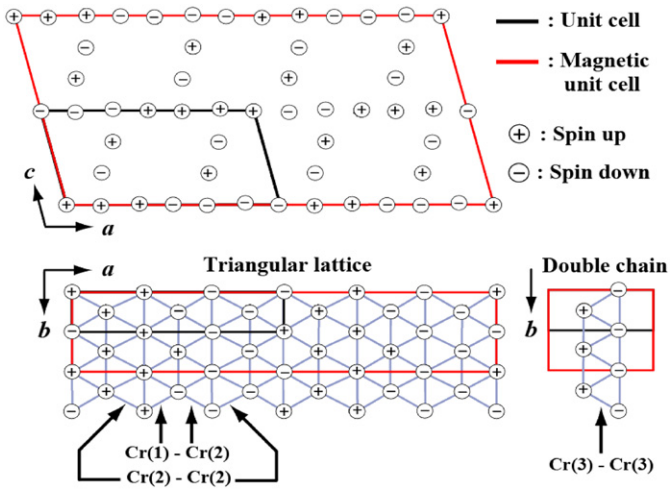

Fig. 10. A model of magnetic structure for $RbCr_5S_8$. A collinear type (spin up and down) is assumed in this model.

a phase shift of antiferromagnetically ordered Cr(1) chains, as shown in Fig. 10. A model of magnetic structure shown in Fig. 10 is constructed on the basis of above mentioned arguments. The simulation of the obtained diffraction pattern with this model gave rather good agreement as a whole, but it was a little bit insufficient in the intensity of individual diffraction peaks. Our simulation was limited to only a collinear type (spin up and down). In real case, however, the magnetic structure may be much complex, for example, spiral, screw or helical order. ND using single crystals is crucial to determine the precise magnetic structure. Other compounds probably have similar magnetic structures, because the essential structural characteristics are similar in all compounds. The most significant difference of the magnetic structures between $RbCr_5S_8$ and $TlCr_5Se_8$ is the absence of the doubling of the *b*-axis in $TlCr_5Se_8$. This might be due to a ferromagnetic interaction along the *b*-axis (Cr–Cr distance with 3.6 Å comparable to Cr(2)–Cr(2) distance of $RbCr_5S_8$) in $TlCr_5Se_8$. The magnetic structure constructed by only ferromagnetic chains along the *b*-axis has no doubling of the *b*-axis.

KCr_5S_8 and $Ba_{0.5}Cr_5S_8$ show low-dimensional behaviors. Any remarkable differences of the lattice parameters and local structures are not recognized among the compounds except $Sr_{0.5}Cr_5S_8$, but the β-angle is significantly large in KCr_5S_8 (Fig. 3). Such a large β-angle might lead to weaker magnetic interaction between the triangular lattices through the double chains. Hence, the observed maximum behavior of $\chi(T)$ might be due to such increasing two-dimensionality. On the other hand, a similar behavior of $Ba_{0.5}Cr_5S_8$ cannot be explained by the same reason, because it has almost the same β-angle as in $RbCr_5S_8$. Here, it should be noted that Ba ions order along the *b*-axis (chain direction) and the obtained structural parameters are averaged in the reduced cell, because diffraction peaks from Ba-ordering have not been observed in powder XRD. In the real lattice, Cr(2)–Cr(3) bonds could have alternating length and angle caused by the ordering of Ba-ions and vacancies. Such alternation might weaken magnetic interaction bridging the triangular lattices, leading to increasing two-dimensionality.

$CsCr_5S_8$ with the largest *A*-cation radius among the compounds has the lowest T_N and the highest f (=28). Such high frustration effect is coincident with the triangular lattices and the double chains formed by rather regular triangles in $CsCr_5S_8$. On the other hand, Cs ions reside in rather narrow tunnels. The structural transition accompanied by the expansion of the lattice may occur to relax the narrowing environment on cooling. In $RbCr_5S_8$ with the second largest Rb ions, the magnetic transition is accompanied by the lattice expansion. Such lattice expansion also might occur to relax any frustration and narrow environment, cooperating with magnetic transition. In $SrCr_5S_8$, Cr(2)–Cr(2) distance is anomalously large. This suggests a stronger ferromagnetic interaction of Cr(2)–Cr(2) bond. The observed ferromagnetic enhancement of $\chi(T)$ could be due to the development of ferromagnetic interaction in the Cr(2)–Cr(2) double chains.

5. Summary

The pseudo-hollandite chromium sulfides, ACr_5S_8 (A=K, Rb, Cs) and $A'_{0.5}Cr_5S_8$ (A'=Sr, Ba), have been synthesized and investigated in structural and magnetic properties. The alkaline and alkaline-earth ions with smaller ionic radii than Sr^{2+} did not form pseudo-hollandite compound. This is probably because such small *A*-cations cannot screen the charged $[Cr_5X_8]^{-1}$ frameworks sufficiently. All the compounds show Curie–Weiss type behaviors of magnetic susceptibility in high-temperature region and fall into antiferromagnetically ordered ground states at lower temperatures. Reflecting any magnetic frustration and/or competition of magnetic interactions in the triangular lattice and the double chain, the Néel temperatures are rather low compared with Weiss temperatures. The frustration effect is much remarkable in $CsCr_5S_8$ with the structure made up of near regular triangles. The manner of magnetic transition is different among the compounds. Both KCr_5S_8 and $Ba_{0.5}Cr_5S_8$ show double transitions around 50 and 60 K, respectively. $RbCr_5S_8$ exhibits a sharp magnetic transition at 42 K, accompanied by magnetoelastic behavior. $CsCr_5S_8$ shows a structural transition around 100 K, followed by an antiferromagnetic transition at 10 K. In $Sr_{0.5}Cr_5S_8$, ferromagnetic interaction first develops below 100 K and finally a three-dimensional antiferromagnetic order takes place at 30 K. These magnetic properties are understood from the structural characteristics. The magnetic structure of $RbCr_5S_8$ has a supercell of $2\times2\times2$, which is different from the known magnetic structure of $TlCr_5Se_8$. A possible magnetic structure is proposed on the basis of plausible magnetic interactions in various Cr–Cr bonds and neutron diffraction data.

Acknowledgments

This work was supported in part by Global COE Program (Chemistry Innovation through Cooperation of Science and Engineering), MEXT, Japan and by a Grant-in-Aid for Scientific Research (no. 19052004) from the Japan Society for the Promotion of Science. The authors sincerely thank H. Ueda for valuable discussion, M. Ichihara for TEM experimental support and M. Nishi for ND experiments and the data analysis.

References

[1] M. Vlasse, L. Fournès, Mater. Res. Bull. 11 (1976) 1527.
[2] W. Bensch, J. Koy, Solid State Commun. 93 (1995) 261.
[3] L. Fournès, M. Vlasse, M. Saux, Mater. Res. Bull. 12 (1977) 1.
[4] W. Bensch, E. Worner, Solid State Ionics 58 (1992) 275.
[5] W. Bensch, E. Worner, M. Muhler, U. Ruschewitz, Eur. J. Solid State Inorg. Chem. 30 (1993) 645.
[6] W. Bensch, E. Worner, P. Hug, Solid State Commun. 86 (1993) 165.
[7] W. Bensch, E. Worner, U. Ruschewitz, Eur. J. Solid State Chem. 110 (1994) 234.
[8] J. Huster, Z. Anorg. Allg. Chem. 447 (1978) 89.
[9] S. Petricek, H. Boller, K.O. Klepp, Solid State Ionics 81 (1995) 183.
[10] F. Izumi, T. Ikeda, Mater. Sci. Forum 198 (2000) 321.
[11] W. Bensch, C. Näther, O. Helmer, C. Ritter, J. Alloys Compd. 290 (1999) 41.
[12] P. Colombet, M. Danot, Solid State Commun. 45 (1983) 311.
[13] P. Colombet, L. Trichet, Solid State Commun. 45 (1983) 317.
[14] J.B. Goodenough, J. Phys. Chem. Solids 6 (1958) 287.
[15] J. Kanamori, J. Phys. Chem. Solids 10 (1959) 87.